ISBN: 978-3-95450-231-8 ISSN: 2673-5490 doi: 10.18429/JACoW-IPAC2023-WEPM100

DESIGN OF PERMANENT MAGNET DIPOLES-QUADRUPOLES WITH LONGITUDINAL GRADIENT FOR THE PETRA IV STORAGE RING

M. Gehlot†, P. N'gotta, T. Ramm, M. Tischer DESY, Hamburg, Germany
J. Chavanne ESRF, Grenoble, France

Abstract

The PETRA IV storage ring is a project planned to replace the Synchrotron light source PETRA III. The main aim is to reduce the horizontal emittance as low as 20 pmrad. This nominal emittance will be achieved by a hybrid six bend achromat lattice (H6BA). The magnets used in this lattice will be a combination of resistive quadrupole magnets and permanent dipole magnets.

The design concept for the dipoles is a further advancement of the ESRF-EBS dipoles with longitudinal gradient. For the PETRA IV lattice, three different types of permanent dipole magnets will be used which include a combined function dipole-quadrupole magnet with both longitudinal and transverse gradient (DLQs). As for all high brilliance light source magnets, there are very demanding field quality requirements for these dipoles. This contribution presents the design details of the permanent magnet-based combined-function dipoles and discusses the expected magnetic field properties obtained from 3D Radia simulations.

INTRODUCTION

The use of permanent magnet (PM) material for magnets in modern multi-bend lattices is particularly advantageous for achieving a compact design but also for reducing the power consumption during operation [1-3]. In the hybrid six-bend achromat lattice (H6BA) for the proposed PETRA IV storage ring [4,5], all bending magnets will be made of permanent magnets, following the successful implementation of permanent magnet dipoles with longitudinal gradient at the ESRF for the previous EBS upgrade [6,7]. Also, the planned SLS-2 upgrade [8] will make extensive use of PM-based magnets, which are currently in production. In fact, all the PETRA IV bending magnets will be combined-function magnets as they will additionally also provide a moderate quadrupole gradient.

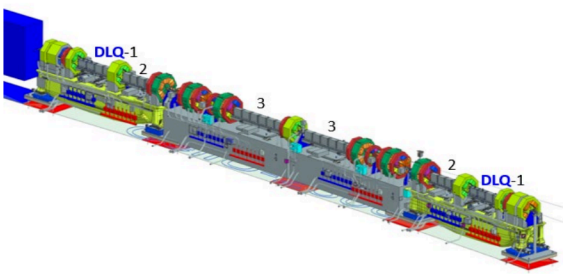

Figure 1: PETRA IV storage ring H6BA lattice showing DLQ-1,2,3 magnets.

† mona.gehlot@desy.de

COMBINED-FUNCTION DIPOLES

Three different types of permanent magnet dipoles will be used in the H6BA cell as illustrated in Fig. 1. Out of three dipole magnets, one has both transverse and longitudinal gradients which is DLQ1. It consists of four modules (M4-M1) with a ~23% stepwise decreasing magnetic field; the field-to-gradient ratio B/G remains, however, constant. The other two magnets, DLQ2 and DLQ3, have only a transverse gradient. DLQ2 has four modules with identical magnetic field amplitude and gradient, and DLQ3 has six modules with identical magnetic field and gradient. Figure 2 shows the cross-section of the DLQs in the magnetic model. The overall design with a C-shaped yoke provides a less constrained design of the photon extraction chamber and an easier installation process of both, DLQs and vacuum chambers. Due to the moderate gradient values in the DLQs (B/G~25.8mm), a modified dipole design with slanted poles is applied resulting in an efficient design with a compact cross-section of about 120×200 mm^2 (w × h). The design studies started with DLQ1, which has higher field and gradient compared to the other types and also provides a higher complexity due to the longitudinal gradient. All solutions found for this magnet can subsequently be directly transferred to the other DLQ types.

For design and manufacturing simplicity, all DLQ1 modules will have the same magnetic gap and pole profile, but will be magnetised by a different number of magnets to adjust the magnetic field strength and gradient to the required values for each module.

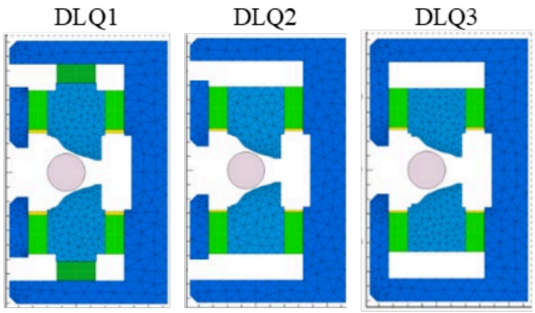

Figure 2: Cross section of combined-function dipoles in the magnetic model; thermal shims (yellow) are placed on top of the permanent magnets (green).

The yoke and poles are made of soft iron. The magnetic material used for the DLQs is SmCo. This PM material has the advantage of higher resistance to radiation damage and lower temperature dependence. The auxiliary pole at the open side of the magnet plays an important role in the magnetic design. The vertical distance between the auxiliary pole and the yoke is different for all three DLQs. In the case

ISBN: 978-3-95450-231-8 ISSN: 2673-5490 doi: 10.18429/JACoW-IPAC2023-WEPM100

of DLQ1, additional top magnets are required in order to generate the higher gradient and field. The target beam position is offset by about -7 mm from the geometric centre of the main pole to achieve the required field amplitude. Fe-Ni thermal shims (yellow stripes in the model of Fig. 2) are provided on the side magnets for thermal stability of the magnets in the presence of unavoidable small temperature drifts in the storage ring tunnel during operation. For further tuning of higher harmonic contents, Fe-Si shims are used on top of the thermal shims (not shown in the model). Table 1 lists the DLQ lattice parameters. The integrated field values for DLQ1, DLQ2, and DLQ3 are -0.314 Tm, -0.204 Tm and -0.348 Tm, respectively, which sums up 2.5° bending angle per half-cell. The related integrated gradient values are -12.3 T, -8.4 T and -11.9 T respectively.

Table 1: Lattice Parameters of PETRA IV DLQ Magnets.

	Magnet length (m)	Field (T)	Gradient (T/m)	Bending angle (rad)
DLQ1	0.303	-0.289	-11.23	0.015
	0.303	-0.277	-10.73	
	0.303	-0.255	-9.89	
	0.303	-0.223	-8.65	
DLQ2	1.084	-0.190	-7.76	0.010
DLQ3	1.808	-0.192	-6.63	0.017

2D-Design Studies for a Single Module:

The Radia software [9] is used for 2D and 3D magnetic simulations. The overall design of poles, yoke and PMs is developed by 2D simulation studies, i.e. excluding all end effects. The required field quality is then obtained using a pole shape optimisation algorithm which flattens the gradient homogeneity within the specified good-field region (GFR) of R=8 mm. Like for other PETRA IV magnets, the

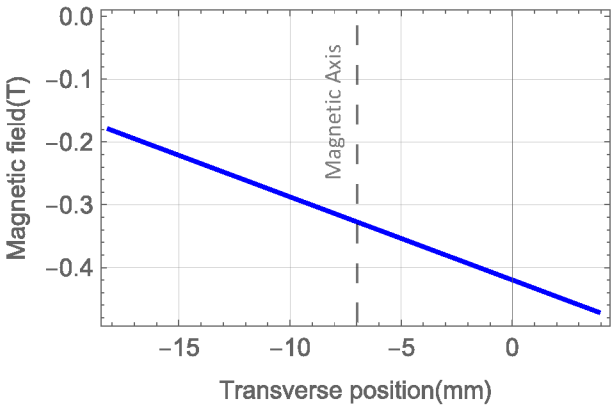

Figure 3: Magnetic field of the DLQ1 high-field module, the magnetic axis is located at -7.05 mm.

remaining field errors are defined as the quadratic sum of all field harmonics $\sqrt{\sum_{i=1}^{N} B_i^2}$ with a maximum value of 5×10^{-4}. The position of the auxiliary pole is important to obtain a sufficiently large GFR and has been found to sensitively drive the sextupole component.

A tuning margin must be included in the magnetic design for field strength and gradient, since a correction of field errors during magnetic measurements can be only done by locally shunting the magnetic circuit. Figure 3 shows the magnetic field of the DLQ1 high-field module in transverse direction, the magnetic axis is located at -7.05 mm. An rms gradient homogeneity of 1.5×10^{-4} has been obtained. The quadratic sum of all field harmonics as a figure of merit is 1.4×10^{-4} inside the required GFR, which is well within the specified limits.

3D-Design Studies for Assembled DLQ1:

Once the required field and gradient were obtained from 2D calculations for a single module, 3D simulations were performed to study the end field effects of a single module and finally the crosstalk between the modules. Figure 4 shows the design of the assembled DLQ1 with the modules placed along the curved path. Thin endpole pieces had been attached at both ends of all modules and slightly reshaped from the nominal pole contour so that they compensate the end effects. For faster optimisation, the field properties were for now evaluated along a straight trajectory through the DLQ. It is known from a previous comparison that an analysis along the real curved trajectory results in a tiny systematic change of the gradient homogeneity with a sextupole of about 1 unit as the largest contribution to be considered in the final design step. Figure 5 shows the homogeneity of the integrated gradient along the transverse position with a standard deviation of 2.3×10^{-4}. The analysis of higher field harmonics, which are normalised to the integrated dipole component, is seen in Fig. 6. The quadratic sum of field harmonics amounts to 1.1×10^{-4}, well within the required specifications. A comparison of the lattice magnetic field with the simulated field in Fig. 7 illustrates the margin of several percent included in the design for field tuning. The dips at the field steps originate from the small 4 mm air gap in between modules which is included for mechanical reasons. Figure 8 shows the gradi-

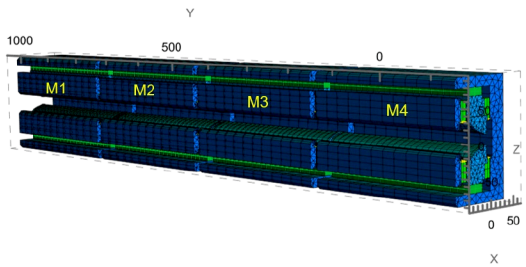

Figure 4: Magnetic model of a full DLQ1.

ISBN: 978-3-95450-231-8 ISSN: 2673-5490 doi: 10.18429/JACoW-IPAC2023-WEPM100

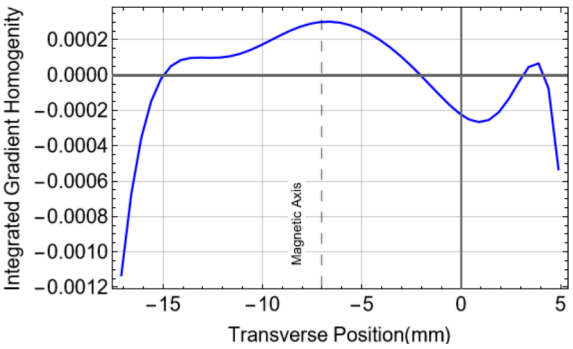

Figure 5: The integrated gradient along transverse position has a homogeneity of 2.3×10^{-4} RMS for DLQ1.

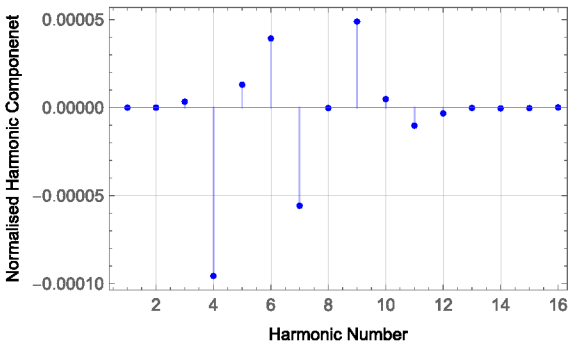

Figure 6: Analysis of higher harmonics (normalised to integrated dipole) results in 1.1×10^{-4} for the quadratic sum of all components.

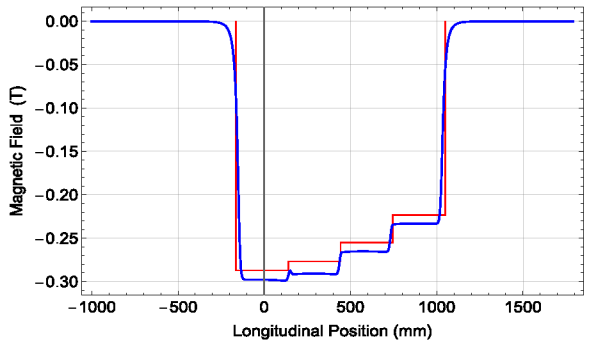

Figure 7: Longitudinal field dependence of DLQ1 as simulated in comparison with lattice values.

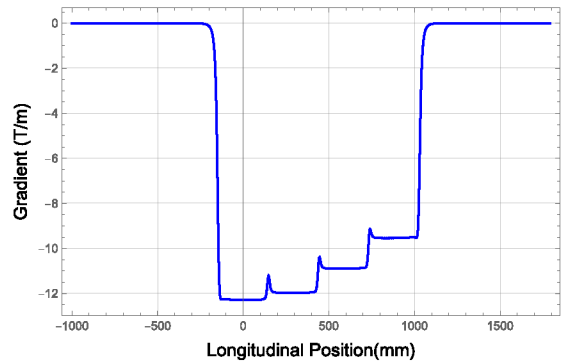

Figure 8: Longitudinal variation of gradient of a full DLQ1, small crosstalk at module breaks is evident.

ent along the longitudinal direction. As expected, the cut-off of the gradient and also the dips between modules, are more pronounced for the quadrupole component than for the field. Further studies on the design of the endpoles are ongoing. Slightly different endpole geometries may finally be used for the extremities of the outer modules and in between two adjacent modules.

CONCLUSION

Three different permanent magnet-based combined-function dipole magnets are presently developed for the PETRA IV storage ring. The DLQ1 type presented in this paper provides also a longitudinal field gradient. The design successfully achieves the required lattice parameters and field quality. The magnetic layout is transferred to a mechanical design for all modules and the complete DLQ1 which will lead to manufacture of a first prototype in near future. The magnetic measurement system for the DLQs will be a stretched wire bench, selection of components is currently under investigation. The compact size and reduction in power consumption and operating costs of PM magnets is a fruitful choice for upcoming future accelerator facilities.

REFERENCES

[1] B. J. A. Shepherd, "Permanent Magnets for Accelerators", in *Proc. IPAC'20*, Caen, France, May 2020, pp. 1. doi:10.18429/JACoW-IPAC2020-MOVIR005

[2] J. Chavanne and G. Le Bec, "Prospects for the use of Permanent Magnets in Future Accelerator Facilities", in *Proc. IPAC'14*, Dresden, Germany, Jun. 2014, pp. 968-973. doi:10.18429/JACoW-IPAC2014-TUZB01

[3] J. Citadini *et al.*, "Sirius—A 3 GeV Electron Storage Ring Based on Permanent Magnets", *IEEE Trans. Appl. Supercond*, vol. 22, pp. 4004404-4004404, 2012. doi:10.1109/TASC.2012.2185771.

[4] R. Bartolini *et al.*, "Status of the PETRA IV Machine Project", in *Proc. IPAC'22*, Bangkok, Thailand, Jun. 2022, pp. 1475-1478.doi:10.18429/JACoW-IPAC2022-TUPOMS029

[5] R. Bartolini *et al.*, "Magnet Design for the PETRA IV Storage Ring", in *Proc. IPAC'22*, Bangkok, Thailand, Jun. 2022, pp. 2767-2769.doi:10.18429/JACoW-IPAC2022-THPOTK002

[6] G. Le Bec *et al.*, "Magnets for the ESRF Diffraction-Limited Light Source Project", *IEEE Trans. Appl. Supercond*, vol. 26, pp. 1-8, 2016. doi:10.1109/TASC.2015.2510402.

[7] C. Benabderrahmane *et al.*, "Status of the ESRF-EBS Magnets", in *Proc. IPAC'18*, Vancouver, Canada, Apr.-May 2018, pp. 2648-2651. doi:10.18429/JACoW-IPAC2018-WEPMK009

[8] H. Braun et al., "SLS 2.0 storage ring technical design report", PSI, Villigen, Switzerland, Rep. 21-02, 2021.

[9] O. Chubar, P. Elleaume, J. Chavanne, Radia developed at ESRF, version 4.1. https://www.esrf.fr/Accelerators/Groups/InsertionDevices/Software/Radia